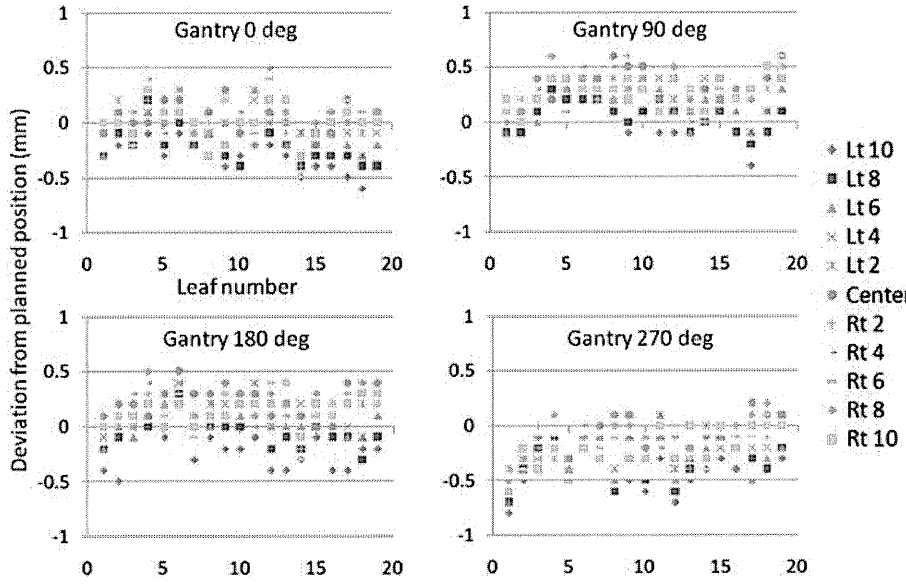

Fig. 5. Deviation from the planned position for four gantry angles at each MLC slit location. The X axis shows leaf number. The Y axis shows deviation from planned position in millimeters. Each symbol shows the MLC abutment location (left 10 cm to right 10 cm with 2-cm interval).

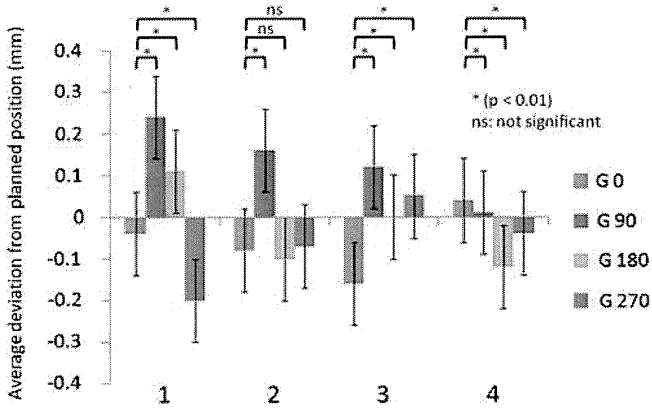

Fig. 6. Average deviations from the planned position at four gantry angles over 1 month. The X axis is measured in weeks. The Y axis shows average deviation from planned position in mm at four gantry angles of 0, 90, 180, 270°. Error bars present one standard deviation. Paired *t*-test comparisons between gantry angle 0° and the other angles are shown ($P < 0.01$: significant difference, ns: not significant).

not based on the influence of gravity; that is, it was not possible to identify patterns of gravity-induced movement of MLC leaf positions toward the floor.

Using the same combination of MLC and EPID for analysis as in the present study, Parent *et al.* [21] reported that measurements at gantry angles of 90 and 270° showed no significant effect of gravity. For gantry angle 90°, a tendency for the error from a planned MLC location to gradually decrease was evident from the first to the fourth time. A similar tendency was seen for gantry angle 270°. We suspect that this tendency was due to the narrowing orientation of the MLC along the central beam axis over this month.

Nongap test

Figure 3 shows the nongap image of measurement at a gantry angle of 0°. The MLC abutment region in white was relatively underdosed compared with the open field area, whereas this region in black was relatively overdosed. There were many underdose regions compared with overdose regions. Figure 7 shows the quantitative data of the pixel ratio at each MLC abutment position. The value of pixel ratio at each MLC abutment region was not the same, most of them were over 100.

Figure 8 shows a comparison of pixel ratio between the first and last data points measured over 1 month at gantry angle 0°. Average pixel ratio was calculated for all leaves at every MLC abutment position (Lt 8–Center–Rt 8). In every MLC abutment position, the variation in pixel ratio was absolutely positive (the change in color white) and showed an intentional trend toward a decrease in dose ($P < 0.001$). Figure 9 shows a change of average pixel ratio measured at every MLC abutment position at gantry angle 0° over 1 month. The value of which was gradually changed to positive for every MLC abutment position. It is thought that the MLC locations became progressively narrowed in the orientation of the central beam axis over 1 month, resulting in underdosing in the overlapping parts of the pixel profiles.

Figure 10 shows a correlation between the average pixel ratios measured at every MLC abutment position at gantry angle 0° and the average deviation from planned position at

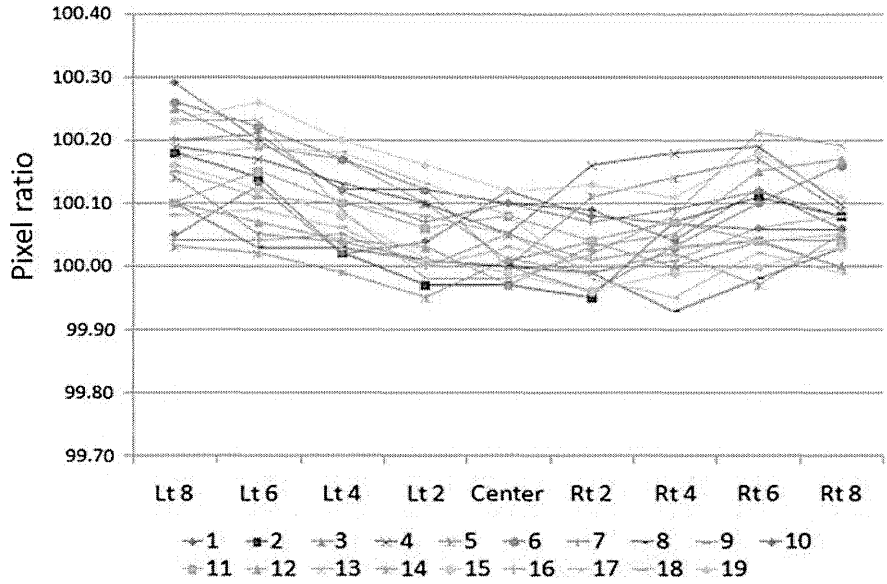

Fig. 7. Pixel ratio at the MLC abutment position for 19 leaves. The X axis shows the MLC abutment position (left 8 cm to right 8 cm with 2-cm interval) and the Y axis shows the pixel ratio at the MLC abutment position for 19 leaves.

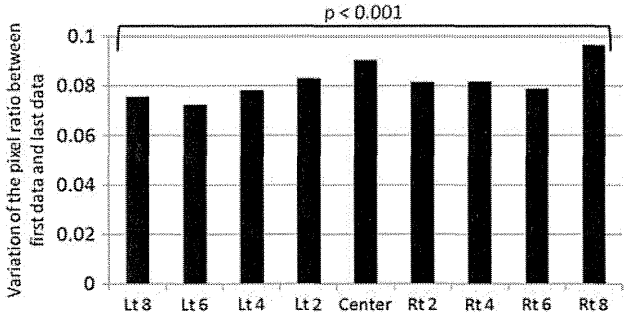

Fig. 8. Change in average pixel ratio between the first and last data points at the MLC abutment position. The X axis shows the MLC abutment position (left 8 cm to right 8 cm with 2-cm interval) and the Y axis shows variation of the pixel ratio between first data and last data. Paired *t*-test comparisons between first data and last data are shown ($P < 0.001$: significant difference for every MLC abutment position).

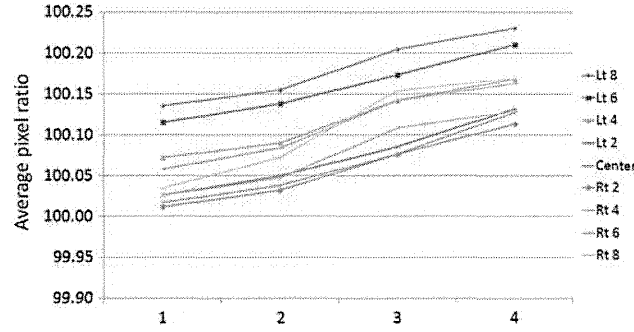

Fig. 9. Change in average pixel ratio at the MLC abutment position over 1 month. The X axis is measured in weeks. The Y axis shows average pixel ratio at the MLC abutment position (left 8 cm to right 8 cm with 2-cm interval).

the same MLC slit location over one month. The data of average pixel ratios are the same as the result of Fig. 9. The data of average deviation from planned position are the same as the result of Fig. 6. Although the value of average pixel ratio was gradually changed positive for every MLC abutment position that mentioned previously in Fig. 9, the average deviations from planned position were distributed between the ranges of –0.30 mm to 0.30 mm.

Figure 11 shows the results of the nongap test, in particular the gantry angle dependency of the initial data obtainedin thet first week. The average pixel value of the abutment section in each MLC location (Lt 8–Center–Rt 8) is shown: in every MLC location, the average pixel ratio is clearly lower (the change in color black) at the other gantry angles than at gantry 0°. This variation was larger at gantry angle 180° than at 90 or 270°. The MLC leaves used in this investigation move in an arc trajectory, giving rise to the phenomenon that the MLC positions spread slightly due to their own weight at gantry angle 180° compared with gantry angle 0°. We consider that this effect explains the increase in overlap in dosage profiles.

DISCUSSION

In this study, we investigated the use of an EPID to conduct quality assurance analysis of MLC leaf position. Palta *et al.* recommended that the tolerance limit of leaf position for segmental MLC should be 1 mm, and this

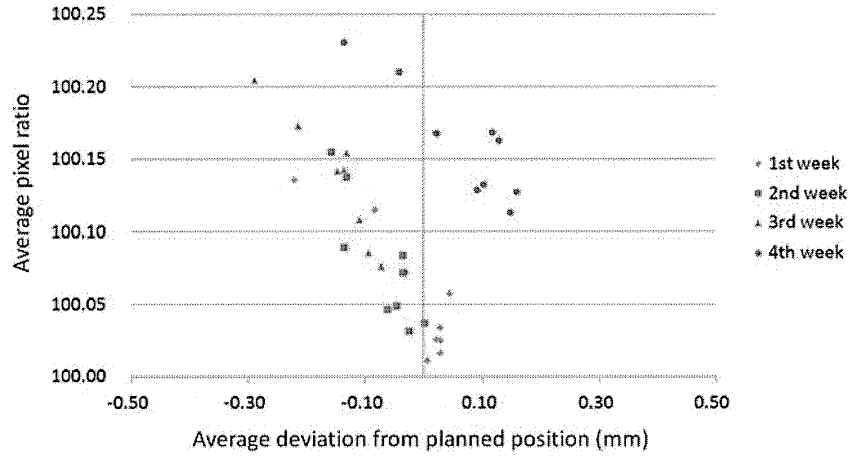

Fig. 10. Average pixel ratio at every gap or slit location against the average deviation from planned position over 1 month. The X axis shows average deviation from planned position in millimeter and the Y axis shows average pixel ratio. Each symbol shows the average pixel ratio at every gap location (left 8 cm to right 8 cm with 2-cm interval) over 1 month.

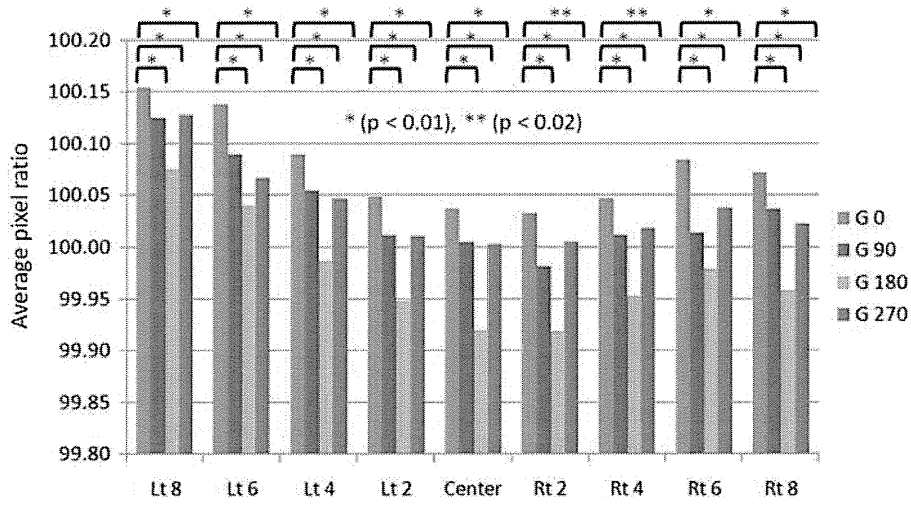

Fig. 11. Average pixel ratio at every gap location as a function of gantry angle. The X axis shows every gap location (left 8 cm to right 8 cm with 2-cm interval). Average pixel ratio was significantly different with a P value < 0.01 (*) or < 0.02 (**) for four gantry angles of 0, 90, 180 and 270°.

restriction should be made smaller than the 1 pixel size of a computed tomography (CT) image [20]. The CT protocol used in our department is set to a pixel size of 0.98 mm with a field of view of 50 cm for 512×512 matrixes. Chang *et al.* also used an EPID with the pixel size of 0.78 mm for verification of leaf position. They mentioned that the garden fence pattern with a slit size of 1 mm can be faithfully reproduced even with a pixel size of 0.78 mm and the accuracy of the QA procedure was not compromised [18]. On this basis, it was judged that the resolution of 0.27 mm/pixel used in this study was small enough for analysis. LoSasso *et al.*'s [22] assessment of leaf precision using alternating dynamic and static fields showed that leaf precision was about 0.25 mm, based on a qualitative assessment of radiographic exposures of overlapping fields. This value was close to that we used here using an EPID. Even if the accuracy of MLC leaf position was within the tolerance limit, the dose between MLC abutment leaves was not always stable because of the change of leaf position error shown in Fig. 6. Therefore the nongap test should be performed continuously to check the change of pixel intensities at the MLC abutment region as shown in Fig. 9. Indeed the average deviation from planned position ranged between –0.30 mm and 0.30 mm, which were within the tolerance limit, the average pixel ratios were gradually changed to positive values over 1 month as shown in

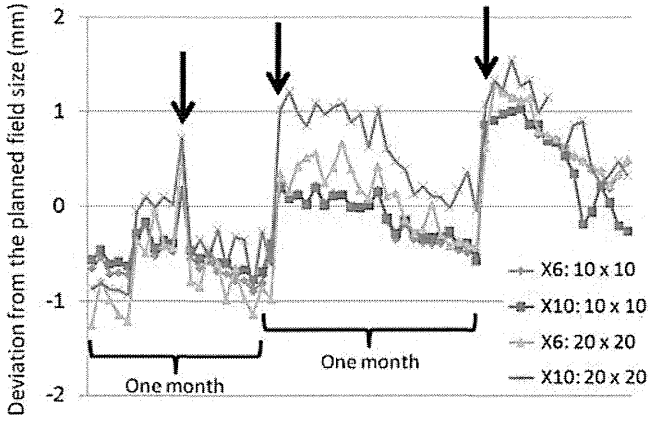

Fig. 12. Deviations from the planned field size of 10 cm × 10 cm and 20 cm × 20 cm over 3 months. The X axis shows the time of measurement. Each symbol shows deviation from the planned field size in mm for energy levels of of 6 and 10 MV, field size of 10 cm × 10 cm and 20 cm × 20 cm, respectively. Arrows indicate MLC calibration periods.

Fig. 10. Even the deviation of leaf position was small, it was possible to confirm pixel ratio sensitively. That is it is insufficient to only perform the garden fence test for the accuracy of MLC leaf positions, and it should also be added that the nongap test should be performed continuously. Since the nongap test uses EPID images, it is easy to perform and possible to evaluate quantitatively with objectivity. Although the pixel intensity was not necessarily identical with the dose, it might be possible that the pixel intensity profile used in the nongap test was substituted for a relative evaluation of overdosing or underdosing generated in the MLC abutment region. In case of the decision as to ROI position in the nongap test, we manually set the ROI at the same position only in the left top corner on the composite image as precisely as possible for every analysis. Even if the ROI position was by a few pixels, the value of the pixel ratio was not drastically changed: 0.03% as a maximum because the ROI has a band of 10 mm × 5 mm.

Figure 12 shows the radiation field size measured daily for both 10 cm × 10 cm and 20 cm × 20 cm fields at energy levels of 6- and 10-MV X-ray over about 3 months.

The vertical axis indicates deviation from the planned field size in millimeters while the arrows indicate when MLC calibration was performed, namely calibration of exposure field size. Every field size showed a tendency to gradually narrow by as much as 1 mm over 1 month. The MLC used in this study is controlled by a potentiometer and an encoder to recognize leaf positions. The potentiometer has an absolute current value and the encoder has a relative value. This linac machine is also equipped with a feature that stops the MLC leaves moving toward the isocenter once the field size changes according to the manufacturer's hardware control system. If the linac system is turned off at the end of the work day and turned on again the following morning, the encoder is initialized. Following initialization, while the absolute current value for the potentiometer of each MLC leaf does not change, the MLC leaf position is moved toward the closing field via integration of the on/off switching procedure of the system. As a result of this phenomenon, periodical MLC calibration should be performed to adjust the discrepancy between the radiation field size and the value recognized by the detector, namely the potentiometer. We established a field size at the time of calibration of 0.5–1.0 mm wider than the planned field size, as shown in Fig. 12. This explains the tendency in the results of Figs 8 and 9 toward a gradual decrease in relative dose intensity at the abutment regions in the nongap test for about 1 month. The MLC calibration procedure is based on manual control, in which the light field created by the MLC leaf position is fitted by the operator to four positions (–10, 0, 10, 20 cm) using millimeter graph paper [23], and variation in this calibration may accordingly be operator-dependent. The garden fence and nongap tests should therefore be performed immediately after MLC calibration to check the results of the manual calibration setting.

In this work we present a fast and accurate method for computing individual MLC leaf positions and relative dose intensities at the MLC abutment region for in-air portal images. Using the XRETIC plate and an EPID, it was possible to analyze MLC leaf position at a resolution of 0.27 mm with the measurement uncertainty of 0.14 mm, and to evaluate relative dose intensity quantitatively at MLC abutment positions. These findings should be of interest in step-and-shoot IMRT. We also characterized the MLC leaves for this type of machine. Namely, MLC leaf positions were gradually contracted with repeated system on/off switching. We therefore confirmed the dosimetric impact of nongap testing and the change in MLC leaf positions. These tests provides dosimetric verification of MLC collimation based on individual leaf position, and have application in patient pretreatment QA of MLC fields and general MLC QA, as well as in checking MLC calibration variation.

REFERENCES

1. Luo W, Li J, Price RA Jr *et al.* Monte Carlo based IMRT dose verification using mlc log files and R/V outputs. *Med Phys* 2006;**33**:2557–64.
2. Woo MK, Nico A. Impact of multileaf collimator leaf positioning accuracy on intensity modulation radiation therapy quality assurance ion chamber measurements. *Med Phys* 2005;**32**:1440–5.
3. Mu G, Ludlum E, Xia P. Impact of MLC leaf position errors on simple and complex IMRT plans for head and neck cancer. *Phys Med Biol* 2008;**53**:77–88.
4. Low DA, Sohn JW, Klein EE *et al.* Characterization of a commercial multileaf collimator used for intensity modulated radiation therapy. *Med Phys* 2001;**28**:752–6.

5. Sastre-Padro MA, van der Heide U, Welleweerd H. An accurate calibration method of the multileaf collimator valid for conformal and intensity modulated radiation treatments. *Phys Med Biol* 2004;**49**:2631–43.
6. Sastre-Padro M, Welleweerd J, Malinen E *et al.* Consequences of leaf calibration errors on IMRT delivery. *Phys Med Biol* 2007;**52**:1147–1156.
7. Vieira SC, Dirkx MLP, Pasma KL *et al.* Fast and accurate leaf verification for dynamic multileaf collimation using an electronic portal imaging device. *Med Phys* 2002;**29**:2034–40.
8. Yang Y, Xing L. Quantitative measurements of MLC leaf displacements using an electronic portal image device. *Phys Med Biol* 2004;**49**:1521–33.
9. Budgell GJ, Zhang Q, Trouncer RJ *et al.* Improving IMRT quality control efficiency using an amorphous silicon electronic portal imager. *Med Phys* 2005;**32**:3267–78.
10. Mamalui-Hunter M, Li H, Low DA. MLC quality assurance using EPID: a fitting technique with subpixel precision. *Med Phys* 2008;**35**:2347–55.
11. Boyer A, Biggs P, Galvin J *et al.* Basic applications of multileaf collimators. Report of the AAPM Radiation Therapy Committee Task Group No. 50. Madison: Medical Physics Publishing, 2001.
12. Klein EE, Hanley J, Bayouth J *et al.* Task group 142 report: quality assurance of medical accelerators. *Med Phys* 2009;**36**:4197–212.
13. Das IJ, Desobry GE, McNeeley SW *et al.* Beam characteristics of a retrofitted double-focused multileaf collimator. *Med Phys* 1998;**25**:1676–84.
14. Chui CS, Spirou S, LoSasso T. Testing of dynamic multileaf collimation. *Med Phys* 1996;**23**:635–41.
15. Bhardwaj AK, Kehwar TS, Chakarvarti SK *et al.* Dosimetric and qualitative analysis of kinetic properties of millennium 80 multileaf collimator system for dynamic intensity modulated radiotherapy treatments. *J Cancer Res Ther* 2007;**3**:23–8.
16. Venencia CD, Besa P. Commissioning and quality assurance for intensity-modulated radiotherapy with dynamic multileaf collimator: experience of the Pontificia Universidad Catolica de Chile. *J Appl Clin Med Phys* 2004;**5**:37–54.
17. Mamalui-Hunter M, Li H, Low DA. MLC quality assurance using EPID: A fitting technique with subpixel precision. *Med Phys* 2008;**35**:2347–55.
18. Chang J, Obcemea CH, Sillanpaa J *et al.* Use of EPID for leaf position accuracy QA of dynamic multi-leaf collimator (DMLC) treatment. *Med Phys* 2004;**31**:2091–6.
19. Bayouth JE, Wendt D, Morrill SM. MLC quality assurance techniques for IMRT application. *Med Phys* 2003;**30**:743–50.
20. Palta JR, Mackie TR. Intensity-modulated radiation therapy: the state of the art. Madison: Medical Physics Publishing, 2003.
21. Parent L, Seco J, Evans PM *et al.* Evaluation of two methods of predicting MLC leaf positions using EPID measurements. *Med Phys* 2006;**33**:3174–82.
22. LoSasso T, Chui CS, Ling CC. Physical and dosimetric aspects of a multileaf collimation system used in the dynamic mode for implementing intensity modulated radiotherapy. *Med Phys* 1998;**25**:1919–27.
23. Siemens Medical Systems, OPTIFOCUS 82 leaf MLC Tuneup Component ONCOR/PRIMUS," 7337731G.

Journal of Radiation Research, 2012, 53, 936–944
doi: 10.1093/jrr/rrs035 Advance Access Publication 17 July 2012

The usefulness of an independent patient-specific treatment planning verification method using a benchmark plan in high-dose-rate intracavitary brachytherapy for carcinoma of the uterine cervix

Yutaka TAKAHASHI[1,2,*], Masahiko KOIZUMI[2], Iori SUMIDA[3], Fumiaki ISOHASHI[1], Toshiyuki OGATA[1,2], Yuichi AKINO[1], Yasuo YOSHIOKA[1], Shintaro MARUOKA[1], Shinichi INOUE[4], Koji KONISHI[1] and Kazuhiko OGAWA[1]

[1]Department of Radiation Oncology, Osaka University Graduate School of Medicine, 2-2 Yamada-oka, Suita, Osaka, Japan
[2]Division of Medical Physics, Oncology Center, Osaka University Hospital, 2-15 Yamada-oka, Suita, Osaka, Japan
[3]Department of Radiology, Osaka University Graduate School of Dental Medicine, 1-8 Yamada-oka, Suita, Osaka, Japan
[4]Department of Medical Technology, Osaka University Hospital, 2-15 Yamada-oka, Suita, Osaka, Japan
*Corresponding author. Tel: 81-6-6879-3482; Email: ytakahashi@radonc.med.osaka-u.ac.jp

(Received 2 March 2012; revised 15 May 2012; accepted 18 May 2012)

To develop an easy independent patient-specific quality assurance (QA) method using a benchmark plan for high-dose-rate intracavitary brachytherapy for cervix cancer, we conducted benchmark treatment planning with various sizes and combinations of tandem-ovoid and tandem-cylinder applications with 'ideal' geometry outside the patient. Two-dimensional-based treatment planning was conducted based on the Manchester method. We predicted the total dwell time of individual treatment plans from the air kerma strength, total dwell time and prescription dose of the benchmark plan. In addition, we recorded the height (dh), width (dw) and thickness (dt) covered with 100% isodose line. These parameters were compared with 169 and 29 clinical cases for tandem-ovoid or tandem-cylinder cases, respectively. With regard to tandem-ovoid cases, differences in total dwell time, dh, dt and dw between benchmark and individual plans were on average $-0.2\% \pm 3.8\%$, -1.0 mm $\pm$ 2.6 mm, 0.8 mm $\pm$ 1.3 mm and -0.1 mm $\pm$ 1.5 mm, respectively. With regard to tandem-cylinder cases, differences in total dwell time, dh_{front} (the distance from tandem tip to tandem ring), dt and dw between benchmark and individual plans were on average $-1.5\% \pm 3.1\%$, -1.5 mm $\pm$ 4.9 mm, 0.1 mm $\pm$ 1.0 mm and 0.2 mm $\pm$ 0.8 mm, respectively. Of two cases, more than 13% differences in total dwell time were observed between benchmark plans and the clinical cases, which turned out to be due to the use of the wrong source position setting. These results suggest that our method is easy and useful for independent verification of patient-specific treatment planning QA.

Keywords: independent verification; treatment planning; Manchester method; benchmark plan; high-dose-rate intracavitary brachytherapy; uterine cervix

INTRODUCTION

Brachytherapy is an essential component of radiotherapy for the carcinoma of uterine cervix and is often combined with external beam radiation therapy (EBRT) for radical treatment. Several studies have suggested that control rates are significantly improved with EBRT and brachytherapy [1, 2]. High-dose-rate (HDR) remote afterloading intracavitary brachytherapy is widely used throughout Asia and Europe [3], and is becoming steadily more common in the USA [4].

The importance of independent verification of dosimetry prior to HDR brachytherapy treatment delivery has been recognized worldwide, and is specified in the guidelines of international regulatory agencies [5]. The Nuclear Regulation Commission (NRC) considers a 20% difference between the prescribed total dose and delivered dose to be a reportable medical event [5]. Thomadsen *et al.* identified 44 medical events in HDR brachytherapy between 1980 and 2001 in data from the NRC and International Atomic Energy Agency [6]. In fact, patients are often required to

wait during treatment planning with an applicator inserted by a radiation oncologist, during which time errors and miscommunications can easily occur. This situation clearly indicates that patient-specific quality assurance (QA), including independent verification of treatment planning and confirmation of applicator geometry, should be done quickly and easily.

Many studies have reported independent verification methods for HDR brachytherapy treatment planning [7–16]. More recent reports have focused on the development of in-house software based on the AAPM TG 43 [17] formulism to calculate the dose at arbitrary points [13–15]. Although such software might be useful for the commissioning of treatment planning systems, human errors in individual treatment planning in clinical practice will not be identified due to the use of the same coordinate system, digitized applicator paths and dose point coordinates as those in the treatment planning system.

Although image-guided intracavitary brachytherapy has been enthusiastically investigated [18], treatment planning based on the Manchester method using two projection radiographs is still used [3]. One of the goals in intracavitary brachytherapy for carcinoma of the uterine cervix is to achieve the same level of consistency as the Manchester method. We have established the Osaka University Protocol based on the Manchester method with some modifications [19]. The goal of our institution is to achieve consistency with our protocol-based benchmark plans.

Here, we propose a very quick, simple and easy patient-specific independent verification method for Manchester method-based treatment planning using benchmark plans to detect human errors and evaluate the quality of the applicator geometry in the patient.

MATERIALS AND METHODS

Creation of benchmark plans

In this study, Fletcher-type (Fletcher-Williamson Asian-Pacific) tandem-ovoid and tandem-cylinder metal applicators (Nucletron International B.V., Veendaal, the Netherlands) were used. Various sizes and combinations of these applicators were constructed by one radiation oncologist with the 'ideal' applicator geometry outside the patient (Fig. 1a and b) and then reviewed by a medical physicist. We constructed eight kinds of tandem-ovoid and six kinds of benchmark plans (Table 1).

Figure 1c shows the 'ideal' geometry of a tandem-ovoid applicator used in our institution. Namely, a flange on the tandem tube is used at the origin, which is the cervical os

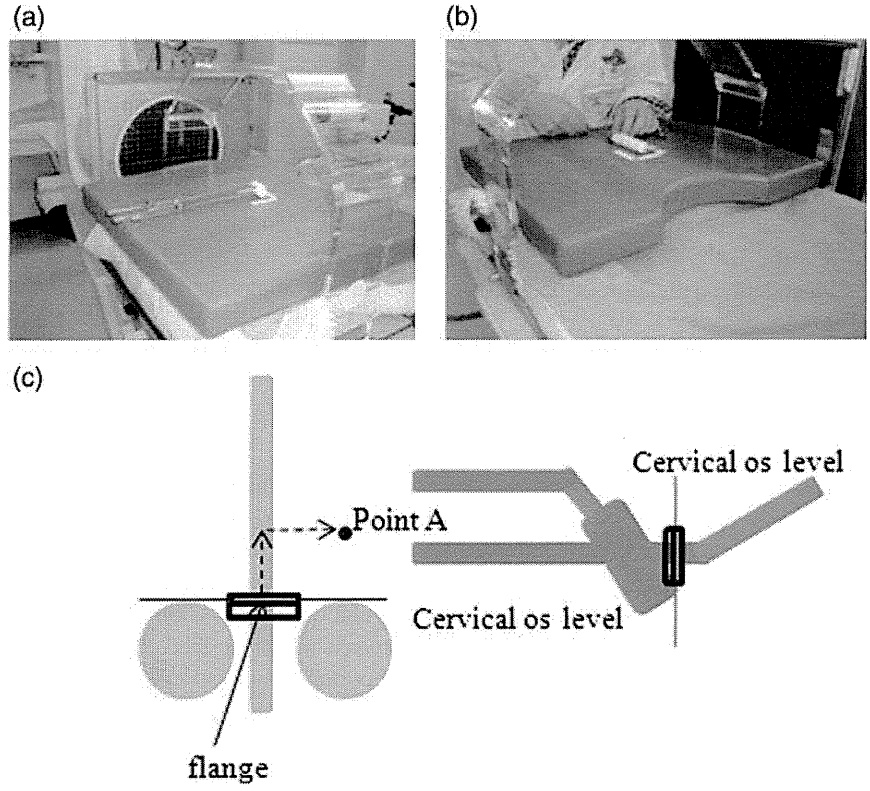

Fig. 1. Creation of benchmark plans. (**a**) Scheme for the construction of tandem-ovoid; (**b**) tandem-cylinder applications; (**c**) typical dose distribution with the tandem-ovoid application.

Table 1. Applicator settings used in benchmark plans

Tandem-ovoid			Tandem-cylinder		
Tandem length (cm)	Ovoid size		Cylinder diameter (cm)		
4	S	SS	2	2.5	3
5	S	SS	N/A	N/A	N/A
6	S	SS	2	2.5	3
7	S	SS	NA	NA	NA

The ovoid diameter of S size is 2.0 cm. The size of SS ovoid is half-cut-size of S ovoid. NA, not applicable.

and the tip of the ovoid is aligned with the origin (a flange on the tandem). Using these ideal applicator settings, treatment planning was performed with PLATO (Nucletron International B.V). Source dwell time was manually optimized based on the Manchester method as demonstrated by Tod and Meredith with minor modification [19–21]. Air kerma strength and total dwell time were then recorded. All benchmark plans were constructed by a medical physicist and reviewed by another medical physicist.

Prediction of total dwell time for individual patient treatments

Dose was calculated with the following formula introduced in AAPM TG43-U1 [22].

$$D(r,\theta) = S_K \times \Lambda \times \frac{G_L(r,\theta)}{G_L(r_0,\theta_0)} \times g_L(r) \times F(r,\theta) \times \text{dwell time} = S_k \times \text{dwell time} \times A$$

where S_K, Λ, G_L, g_L and F represent air kerma strength, dose rate constant, geometric function, radial dose function and anisotropy function, respectively. Here, we defined A as the product of Λ, G_L, g_L (r) and F (r, θ).

The dose at the reference point in the benchmark plan is therefore calculated by the following:

$$D(r,\theta)_b = A_b \times S_{K\_b} \times \text{dwell time}_b \quad (1)$$

Similarly, the dose at point A in the individual plan is calculated by the following:

$$D(r,\theta)_t = A_b \times S_{K\_t} \times \text{dwell time}_t \quad (2)$$

If the 'ideal' tandem-ovoid geometry is achieved in the patient without any planning errors or misuse of the applicator, A_b is nearly equal to A_t. Dwell time in the individual plan can therefore be predicted by the following formula from (1) and (2):

$$\text{Dwell time}_t = \frac{D(r,\theta)_t \times S_{K\_b} \times \text{dwell time}_b}{D(r,\theta)_b \times S_{K\_t}} \quad (3)$$

where $D(r, \theta)_t$ and $D(r, \theta)_b$ represent the prescription dose of each treatment and the benchmark plan, respectively.

Comparison of dose shape with that of the benchmark plans

ICRU report 38 [23] recommends reporting the reference volume as well as total reference air kerma strength and absorbed dose at reference points. The reference volume is the volume encompassed by the reference isodose surface, which is represented by the major dimensions of the following:

(i) Height (dh), which is the maximum dimension along the tandem source measured on an 'oblique' sagittal plane;
(ii) Thickness (dt), which is the maximum dimension perpendicular to the tandem sources measured on a transverse plane;
(iii) Width (dw), which is the maximum dimension perpendicular to the tandem sources measured on a transverse plane.

In addition to the above parameters, we defined the dimensions of dh_{front} and dh_{ext}, which represent the distance from th 100% isodose line of the tip side of the tandem to the origin and that from the 100% isodose line of the connector side of the tandem to the origin, respectively (Fig. 2c).

Figure 2 shows the definitions of these parameters. For the tandem-cylinder, we recorded the additional parameters of dh_{front} and dh_{ext}, which represent the maximum dimension of the 100% isodose line of the tip side of the tandem to the tandem flange, and that of the connector side of the tandem to the tandem flange (Fig. 2c). These values were measured for individual treatment plans and compared with those of the benchmark plans.

Analysis of clinical cases

We retrospectively analyzed 168 and 29 clinical cases from 2009 through 2010 with a tandem-ovoid and tandem-cylinder, respectively. The difference in total dwell time between a benchmark plan and an individual treatment plan was calculated using the following formula:

$$\text{Relativedifference}(\%) = \frac{T_{\text{individual}} - T_{\text{benchmark}}}{T_{\text{benchmark}}} \times 100$$

where $T_{benchmark}$ and $T_{individual}$ represent the total dwell time of the benchmark and individual plans, respectively. Differences in dose distribution shapes, including dh or dh_{front}, and dh_{ext}, dt, and dw between the benchmark and

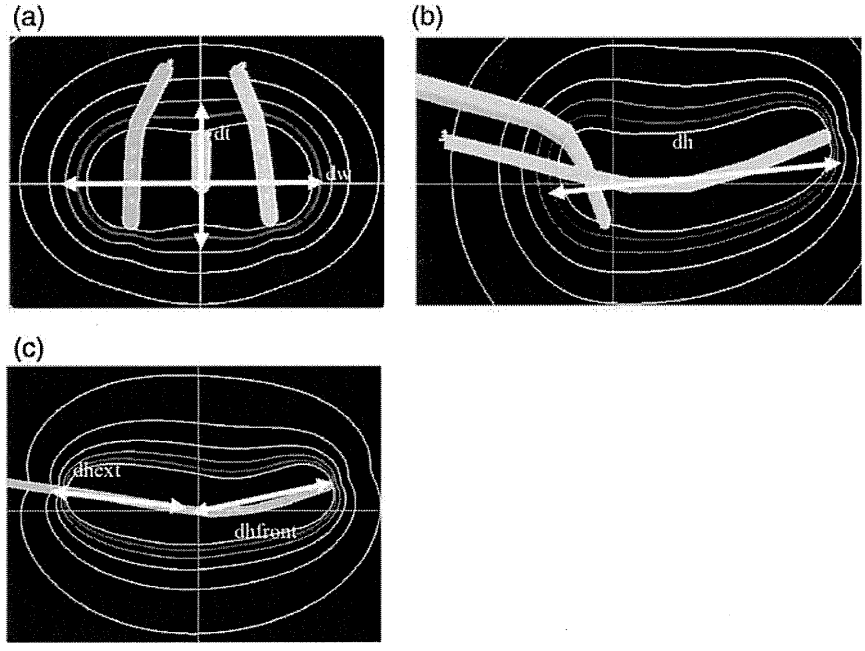

Fig. 2. Definitions of dh, dhfront, dhext, dt and dw used in this study based on ICRU report 38 [23]. These parameters were defined in the plane of the cervical os. (**a**) Transverse plane of tandem-ovoid case; (**b**) sagittal plane of tandem-ovoid case; (**c**) sagittal plane of tandem-cylinder case. Red line shows the isodose line of 100% of the prescription dose.

individual plans were calculated using the following formula:

$$\text{Relativedifference} = \text{shape}_{\text{benchmark}} - \text{shape}_{\text{individual}}$$

Where $\text{shape}_{\text{benchmark}}$ and $\text{shape}_{\text{individual}}$ represent the dose distribution shapes of the benchmark and individual treatment plans, respectively.

Correlations between the differences in total dwell time and those in dh, dt or dw among the benchmark and individual treatment plans were evaluated by Spearman's rank correlation coefficient using Dr. SPSS II software (IMB, New York, USA).

Tolerance levels for total dwell time, dh or dh_{front}, and dh_{ext}, dt, and dw were calculated by the following formula, which was first proposed by Venselaar *et al.* [24]

Tolerance level = mean deviation ± 1.96 SD

RESULTS

Tandem-ovoid cases

Prediction of total dwell time for individual treatment plans

Figure 3 shows a histogram of differences in total dwell time between benchmark and individual treatment plans.

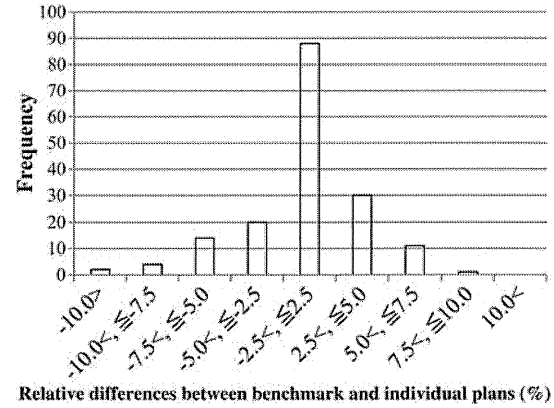

Fig. 3. Histogram of % differences in total dwell time between the benchmark and individual treatment plans.

Differences averaged –0.2% ± 3.8% (range, –13.3–9.6%), and exceeded 5% in 23 of 169 clinical cases.

Comparison of the dose distribution shapes of individual treatment plans with those of the benchmark plans

Figure 4 shows a histogram of differences in dose distribution shapes between the benchmark and individual treatment plans in tandem-ovoid applications. The differences in

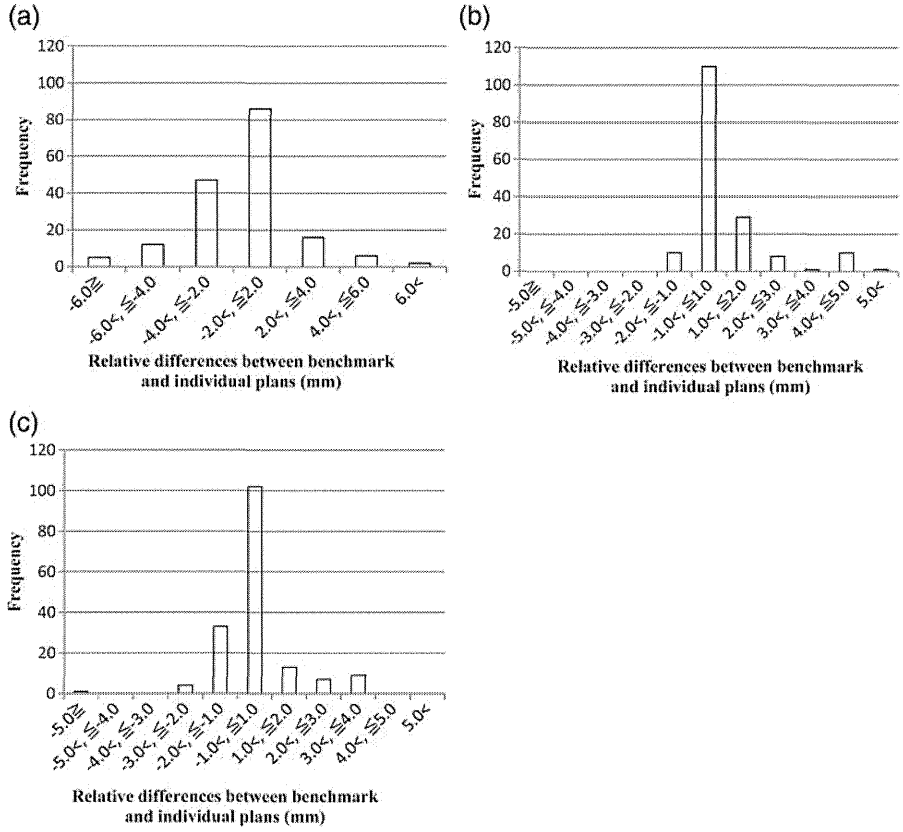

Fig. 4. Histogram of differences in (**a**) dh, (**b**) dt and (**c**) dw between the benchmark and individual treatment plans in mm.

dh, dt and dw between the benchmark and individual plans averaged –1.0 mm ± 2.6 mm (range, –8.6 mm to +6.5 mm), 0.8 mm ± 1.3 mm (range, –1.4 mm to +5.2 mm) and –0.1 mm ± 1.5 mm (range, –5.1 mm to +4.0 mm), respectively.

Regarding dh, 9 of 169 cases showed a difference between the benchmark and individual plans of greater than 5 mm. For dt and dw, in contrast, only one case showed a difference of more than 5 mm.

Subset analysis of cases with large deviations between the benchmark and individual treatment plans

We verified that all tandem-ovoid treatment plans were appropriately created without any planning errors, including wrong source position, wrong decay correction of source strength and inappropriate optimization or use of an unplanned size or combination of applicators. However, 24 of 169 cases had a >5% difference in total dwell time. To explain these differences, we investigated the correlation between differences in total dwell times and dh, dt and dw between the benchmark and individual plans. Figure 5a shows the relationship of differences in total dwell time (vertical axis) with those in dh (horizontal axis). Spearman's rank correlation coefficient ($r_s = 0.836$, $P < 0.01$) showed a strong relationship between the discrepancy in total dwell time and those in dh. In contrast, no correlations were found between the discrepancy in total dwell time and those in dt ($r_s = 0.371$, $P = 0.075$) or dw ($r_s = 0.290$, $P = 0.149$) (Fig. 5b and c).

Tandem-cylinder cases

Figure 6a shows differences in total dwell time between the benchmark and individual treatment plans. Differences averaged –1.5% ± 3.1% (range, –13.0% to +0.4%), with 2 of 29 cases exceeding 11%.

Figure 6b shows the differences in dh_{front}, dh_{ext}, dt and dw between the benchmark and individual treatment plans. Differences averaged –1.5 mm ± 4.9 mm (range, –19.0 mm to +4.0 mm), +1.8 mm ± 5.2 mm (range, –2.2 mm to +20.8 mm), +0.1 mm ± 1.0 mm (range, –1.3 mm to +4.3 mm) and +0.2 mm ± 0.8 mm (range, –0.4 mm to +3.9 mm), respectively. The differences in 2 of 29 cases, which also exceeded an 11% difference in total dwell time, exceeded –19 mm and +20 mm for dh_{front} and dh_{ext}, respectively. These cases were found to have been treated

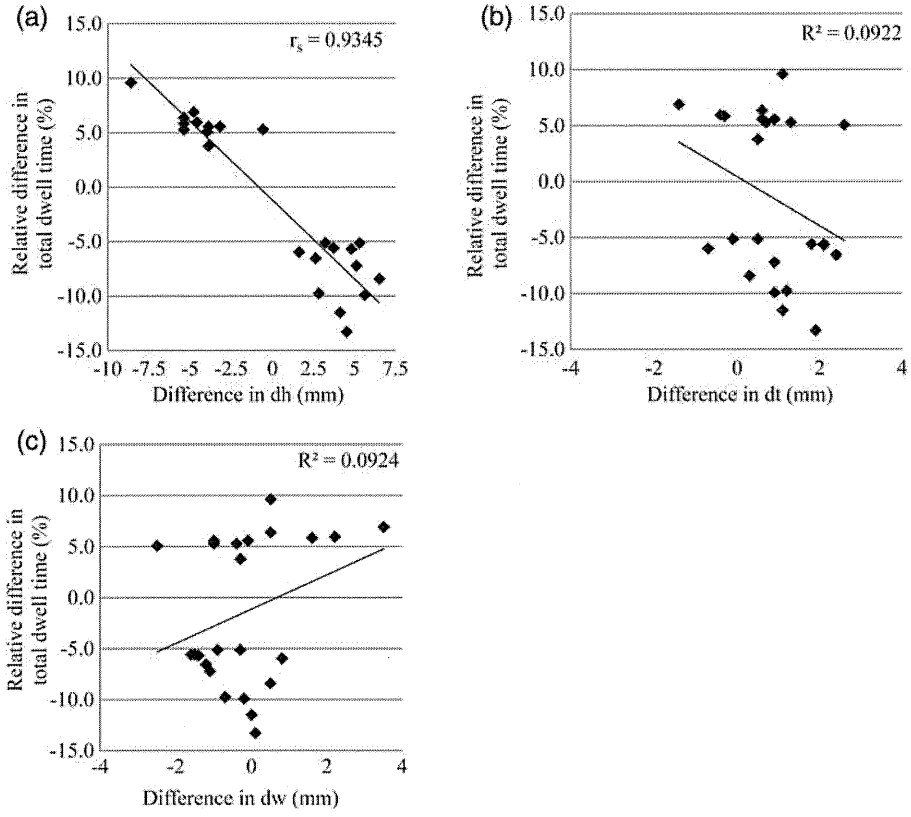

Fig. 5. Correlations between the differences in total dwell time and in (**a**) dh, (**b**) dt and (**c**) dw. Vertical axis shows the % differences in total dwell time between the benchmark and individual treatment plans, and the horizontal axis shows the differences in dh, dt or dw in mm between the benchmark and individual treatment plans.

with an unplanned tandem length, resulting in an incorrect setting for the source dwell positions in treatment planning.

Determination of tolerance limit

For tandem-ovoid cases, the tolerance level of total dwell time, dh, dt, and dw were –7.5% to +7.2, –6.0 mm to +4.1 mm, –1.8 mm to +3.4 mm and –3.0 mm to +2.8 mm, respectively (Fig. 7a).

For tandem-cylinder cases, two cases were excluded from the determination of tolerance limits because they were human error-related. Tolerance limits for total dwell time, dh_{front}, dh_{ext}, dt, and dw were –2.5% to +1.1%, –2.6 mm to +2.3 mm, –2.2 mm to +3.0 mm, –0.9 mm to +0.6 mm and –0.4 mm to +0.4 mm, respectively (Fig. 7b).

DISCUSSION

We used benchmark plans to establish a highly simple, easy, and fast independent treatment planning verification method for high-dose-rate intracavitary brachytherapy for carcinoma of the uterine cervix that requires no special skills such as developing TG43-based in-house software. Despite its great simplicity, analysis of a large number of clinical cases showed that our method was able to detect human error-related planning mistakes, and to evaluate the quality and consistency of applicator geometry.

The Manchester method, which was first suggested by Tod and Meredith in 1938, has been the most broadly used for the treatment of carcinomas of the uterine cervix, with some modifications from the original [20, 21]. They demonstrated an 'ideal' system in which loading patterns of milligrams of radium were determined based on the size of the tandem and ovoids to achieve as constant a dose rate at point A as possible, no matter what combination of applicators was used, and to ensure a suitable ratio between the intra-uterine and vaginal contribution [21]. This rule has been applied to high-dose-rate brachytherapy with an Ir-192 stepping source by modulating the weight of dwell times. In our institution, manual optimization in treatment planning is also based on the Manchester method with some modifications [19]. In addition, the applicator is set such that its geometry is consistent with the 'ideal' geometry specified in the benchmark plan. If there were any planning errors and inappropriate applicator setting, total

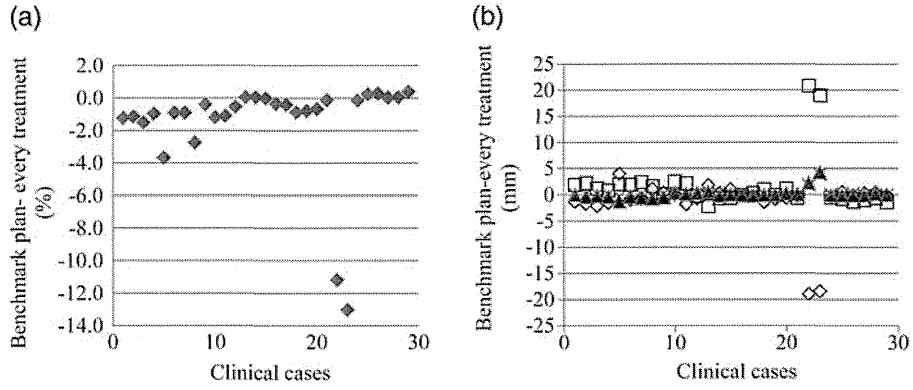

Fig. 6. Differences in (**a**) total dwell time, and (**b**) dh_{front}, dh_{ext}, dt and dw between the benchmark plans and clinical cases in tandem-cylinder settings. White squares, dh_{ext}; white diamonds, dh_{front}; black triangles, dt; and crosses, dw.

dwell time and dose distribution shapes, including dh, dt and dw, in individual treatment plans should agree with those of the benchmark plan. From these points, we established a method for the independent verification of patient-specific treatment planning QA by comparing benchmark plans with individual treatment plans.

Several other independent verification methods for individual treatment planning have been reported. Kumar *et al.* developed an in-house application that calculates the dose at arbitral points [13]. Lachaine *et al.* also developed an in-house application that achieves very fast calculation of point dose [14]. Such kind of applications are likely to be useful in the commissioning of treatment planning systems and partly also in individual treatment planning QA in terms of parameters such as source strength, treatment date and source table, which users input by themselves. However, because these applications use the same Cartesian coordinate system, digitized applicator paths and dose point coordinates as those in the treatment planning system, they are unable to detect human errors associated with the treatment planning process, such as setting of prescription point (Point A) with the wrong coordinate, the incorrect digitization of applicators, incorrect dose points or applicator points, improper magnification of simulation films, or use of an unplanned size or combination of applicators.

Several groups have previously proposed a method of checking total dwell time as a fraction of treatment length and dose prescription, or dose area index for planar implants and single catheter interstitial brachytherapy [8–11]. Recently, for example, Das *et al.* reported that total dwell time can be predicted from the reference volume covered with the prescribed dose (V100) in both single catheter and multiple catheter interstitial implants by the retrospective analysis of V100 from many clinical cases [12]. All these reports were focused on interstitial implants rather than intracavitary brachytherapy, however, and little information on intracavitary brachytherapy for carcinoma of the uterine cervix is available. In 1992, Thomadsen *et al.* demonstrated a method that assures the consistency of dwell times and dose distribution with previous treatment fractions and

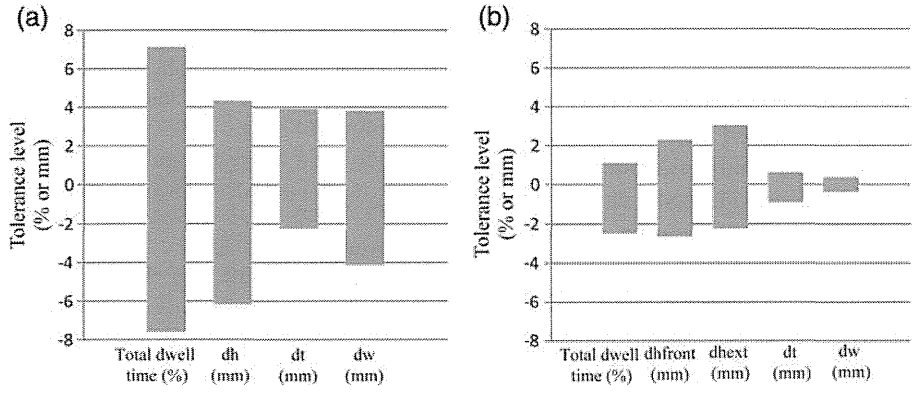

Fig. 7. Tolerance levels of (**a**) tandem-ovoid and (**b**) tandem-cylinder.

previous patients [7]. Although our method is basically similar to their concepts, we created benchmark plans in which the 'ideal' geometry of the tandem-ovoid or tandem-cylinder can be achieved because these applications are constructed outside the patient's body. Therefore the geometry of the applicator can be evaluated in every treatment by comparison with that of the 'ideal' geometry in the benchmark plan.

Although many independent verification methods have been reported, as described above, our present study is one of only a few to evaluate the usefulness of the method in a large number of clinical cases of intracavitary brachytherapy. In tandem-cylinder cases, two cases were found to have >11% differences in total dwell time between the benchmark and individual treatment plans, and >18 mm differences in dh_{front} and dh_{ext}. Review of these two cases showed that these differences were due to the unplanned use of tandem length, which resulted in the use of incorrect settings for the source dwell positions in treatment planning. The results clearly demonstrate that our method can easily identify such kinds of human error.

Regarding tandem-ovoid cases, a thorough review revealed no human-related planning errors. We next examined the reason why 24 cases of tandem-ovoid cases had >5% differences in total dwell time between the benchmark and individual plans. We found that these differences strongly correlated with differences in dh (Fig. 6), indicating that when the ovoid position shifts cranially compared with the benchmark plan, total dwell time decreases because the distance between the sources in the ovoids and point A becomes shorter. Conversely, if the ovoid position shifts caudally to the tandem flange compared with the benchmark plan, total dwell time increases, because the distance between sources in the ovoids and point A becomes larger. These facts indicate that our method is useful in not only finding human errors and software bugs but also in evaluating the quality of the applicator insertion technique. In other words, the evaluation of both the differences in total dwell time and dh could provide a good indicator for the quality of the applicator's geometry.

We set tolerance limits for differences in total dwell time and dose shape between the benchmark and individual treatment plans. Ezell *et al.* reported that they set action levels for per-patient intensity modulated radiation therapy verification using confidence limits [25], as first proposed by Venselaar *et al.* [24]. If the confidence limit is established with sufficient points to provide good statistics, then the value of 1.96σ suggests that variations in excesses of the limit would occur about 5% of the time. We determined the tolerance limits by using confidence limits for total dwell time, dt, dh (dh_{front}, and dh_{ext} for tandem-cylinder cases) and dw. To calculate tolerance limits, we excluded the two cases with >18% differences in tandem-cylinder cases to eliminate the effect of human error-related planning mistakes. These tolerance limits might be one indicator in the evaluation of individual treatment plans (i.e. rechecking of treatment planning, use of appropriate size of applicators, inappropriate applicator geometry, etc.).

One limitation of our study warrants mention, namely that our method is useful only for Manchester-based intracavitary brachytherapy. For carcinoma of the uterus, however, most treatment centers in the world have followed a traditional concept based on the Manchester loading patterns [3, 26]. Moreover, local control rates are significantly improved with EBRT and brachytherapy based on the Manchester method [1]. Our method therefore appears useful despite this limitation.

In conclusion, we established a highly simple, easy and quick independent verification method using benchmark plans for intracavitary brachytherapy based on the 2D-based Manchester method. Despite the great simplicity, our method can evaluate the quality of the applicator insertion technique, as well as identify human errors in treatment planning.

ACKNOWLEDGEMENTS

This study was supported by Grants-in-Aid for Scientific Research (22791194) from the Japan Society for the Promotion of Science. This study was also supported by the Japanese Society of Therapeutic Radiology and Oncology and Grants-in-Aid for Cancer Research (Nos. 23-3-3rd Term Cancer Control-General-007) from the Ministry of Health, Labor and Welfare of Japan.

REFERENCES

1. Lanciano RM, Martz K, Coia LR *et al.* Tumor and treatment factors improving outcome in stage III-B cervix cancer. *Int J Radiat Oncol Biol Phys* 1991;**20**:95–100.
2. Montana GS, Fowler WC, Varia MA *et al.* Carcinoma of the cervix, stage III. Results of radiation therapy. *Cancer* 1986;**57**:148–54.
3. Toita T. Current status and perspectives of brachytherapy for cervical cancer. *Int J Clin Oncol* 2009;**14**:25–30.
4. Nag S, Orton C, Young D *et al.* The American brachytherapy society survey of brachytherapy practice for carcinoma of the uterine cervix in the United States. *Gynecol Oncol* 1999;**73**:111–8.
5. NRC. US Nuclear Regulatory Commission. Title 10, Chapter 1, *Code of Federal Regulations d Energy. Part 35. Medical Use of By-product Material.* Washington, DC: Government Printing office, 2003.
6. Thomadosen BR, Lin SW, Laemmrich P *et al.* Analysis of treatment delivery error in brachytherapy using formal risk analysis techniques. *Int J Radiat Oncol Biol Phys* 2003; **57** (5):1492–508.
7. Thomadosen BR, Shahabi S, Stitt JA *et al.* High dose rate intracavitary brachytherapy for carcinoma of the cervix: The

Madison system: II. Procedural and physical considerations. *Int J Radiat Oncol Biol Phys* 1992;**24**:349–57.
8. Venselaar JLM, Bierhuizen HWJ, Klop R. A method to check treatment time calculations in Ir-192 high dose rate volume implants. *Med Phys* 1996;**22**:1499–500.
9. Ezzell GA. Quality assurance of treatment plans for optimized high dose rate brachytherapy planar implants. *Med Phys* 1994;**21**:659–61.
10. Rogus RD, Smith MJ Kubo HD. An equation to QA check the total treatment time for single-catheter HDR brachytherapy. *Int J Radiat Oncol Biol Phys* 1998;**40**:245–8.
11. Kubo HD. Verification of treatment plans by mathematical formulas for single catheter HDR brachytherapy. *Med Dosim* 1992;**17**:151–5.
12. Das RK, Bradley KA, Nelson IA *et al.* Quality assurance of treatment plans for interstitial and intracavitary high-dose-rate brachytherapy. *Brachytherapy* 2006;**5**:56–60.
13. Kumar R, Sharma SD, Vijaykumar C *et al.* A dose verification method for high-dose-rate brachytherapy treatment plans. *J Cancer Res Ther* 2008;**4**(4):173–7.
14. Lachaine ME, Gorman JC, Palisca MG. A fast independent dose check of HDR plans. *J Appl Clin Med Phys* 2003;**4**(2):149–55.
15. Cohen GN, Amols HI, Zaider M. An independent dose-to-point calculation program for the verification of high-dose-rate brachytherapy treatment planning. *Int J Radiat Oncol Biol Phys* 2000;**48**(4):1251–8.
16. Bidmead M, Briot E, Burger J *et al.* Quality assurance of brachytherapy treatment planning system. In: Venselaar J, Calatayud JP (eds) *A Practical Guide to Quality Control of Brachytherapy Equipment*. Brussels: ESTRO, 2004, 215–31.
17. Nath R, Anderson L, Luxton G *et al.* Dosimetry of interstitial brachytherapy sources: recommendations of the AAPM Radiation Therapy Committee Task Group No. 43. *Med Phys* 1995;**22**:209–34.
18. Toita T, Kodaira T, Shinoda A *et al.* Patterns of radiotherapy practice for patients with cervical cancer (1999–2001): patterns of care study in Japan. *Int J Radiat Oncol Biol Phys* 2008;**70**:788–94.
19. Teshima T, Inoue T, Ikeda H *et al.* High-dose-rate versus low-dose-rate intracavitary therapy for carcinoma of the uterine cervix. Final results of Osaka University Hospital. *Cancer* 1993;**72**:2409–14.
20. Tod M, Merdith W. Treatment of cancer of the cervix uteri, a revised Manchester method. *Br J Radiol* 1953;**26**:252–7.
21. Tod M, Merdith W. A dosage system for use in the treatment of cancer of the uterine cervix. *Br J Radiol* 1938;**11**:809–24.
22. Rivard M, Coursey B, DeWerd L *et al.* Update of AAPM Task Group No.43 Report: a revised AAPM protocol for brachytherapy dose calculations. *Med Phys* 2004;**31**:633–74.
23. ICRU, International Commission on Radiation Units, Measurements. Dose and Volume Specification for Reporting Intracavitary Therapy in Gynecology, *ICRU Report No. 38*. Bethesda, MD: ICRU, 1985.
24. Venselaar J, Welleweerd H, Mijnheer B. Tolerances for the accuracy of photon beam dose calculation of treatment planning system. *Radiother Oncol* 2001;**60**:191–201.
25. Ezzel GA, Burmeister JW, Dogan N. IMRT commissioning: multiple institution planning dosimetry comparisons a report from AAPM task group 119. *Med Phys* 2009;**36**(11):5359–73.
26. Jamema SVJ, Kirisits C, Mahantshetty U *et al.* Comparison of DVH parameters and loading patterns of standard loading, manual and inverse optimization for intracavitary brachytherapy on a subset of tandem/ovoid cases. *Radiother Oncol* 2010;**97**:501–6.

Journal of Radiation Research, 2012, 53, 710–721
doi: 10.1093/jrr/rrs028 Advance Access Publication 5 July 2012

Japanese structure survey of radiation oncology in 2009 based on institutional stratification of the Patterns of Care Study

Teruki TESHIMA[1,*], Hodaka NUMASAKI[1], Masamichi NISHIO[2,*], Hiroshi IKEDA[3], Kenji SEKIGUCHI[4], Norihiko KAMIKONYA[5], Masahiko KOIZUMI[6], Masao TAGO[7], Yutaka ANDO[8], Nobuhito TSUKAMOTO[9], Atsuro TERAHARA[10], Katsumasa NAKAMURA[11], Masao MURAKAMI[12], Mitsuhiro TAKAHASHI[13] and Tetsuo NISHIMURA[14], Japanese Society for Therapeutic Radiology and Oncology Database Committee

[1]Department of Medical Physics & Engineering, Osaka University Graduate School of Medicine, Suita, Osaka, Japan
[2]Department of Radiology, National Hospital Organization Hokkaido Cancer Center, Sapporo, Hokkaido, Japan
[3]Department of Radiation Oncology, Sakai City Hospital, Sakai, Osaka, Japan
[4]Department of Radiation Oncology, St. Luke's International Hospital, Tokyo, Japan
[5]Department of Radiology, Hyogo College of Medicine, Nishinomiya, Hyogo, Japan
[6]Oncology Center, Osaka University Hospital, Suita, Osaka, Japan
[7]Department of Radiology, Teikyo University School of Medicine University Hospital, Mizonokuchi, Tokyo, Japan
[8]Research Center Hospital for Charged Particle Therapy, National Institute of Radiological Sciences, Chiba, Japan
[9]Department of Radiation Oncology, Saiseikai Yokohamashi Tobu Hospital, Yokohama, Kanagawa, Japan
[10]Department of Radiology, Toho University Omori Medical Center, Tokyo, Japan
[11]Department of Clinical Radiology, Kyushu University Graduate School of Medical Sciences, Fukuoka, Japan
[12]Hyogo Ion Beam Medical Center, Shingu, Hyogo, Japan
[13]Department of Radiology, Kiryu Kosei General Hospital, Kiryu, Gunma, Japan
[14]Division of Radiation Oncology, Shizuoka Cancer Center, Shizuoka, Japan
*Corresponding author. Teruki Teshima, MD, Department of Medical Physics & Engineering, Osaka University Graduate School of Medicine, 1-7 Yamadaoka, Suita, Osaka 565-0871, Japan. Tel: +81-6-6879-2570; Fax: +81-6-6879-2570; Email: teshima@sahs.med.osaka-u.ac.jp

(Received 25 March 2012; revised 4 May 2012; accepted 7 May 2012)

The ongoing structure of radiation oncology in Japan in terms of equipment, personnel, patient load and geographic distribution was evaluated in order to radiation identify and improve any deficiencies. A questionnaire-based national structure survey was conducted from March 2010 to January 2011 by the Japanese Society for Therapeutic Radiology and Oncology (JASTRO). These data were analyzed in terms of the institutional stratification of the Patterns of Care Study (PCS). The total numbers of new cancer patients and total of cancer patients (new and repeat) treated with radiation in 2009 were estimated at 201,000 and 240,000, respectively. The type and numbers of systems in actual use consisted of Linac (816), telecobalt (9), Gamma Knife (46), ^{60}Co remote afterloading system (RALS) (29) and ^{192}Ir RALS systems (130). The Linac systems used dual energy function for 586 (71.8%), 3DCRT for 663 (81.3%) and IMRT for 337 units (41.3%). There were 529 JASTRO-certified radiation oncologists (ROs), 939.4 full-time equivalent (FTE) ROs, 113.1 FTE medical physicists and 1836 FTE radiation therapists. The frequency of interstitial radiation therapy use for prostate and of intensity-modulated radiotherapy increased significantly. PCS stratification can clearly identify the maturity of structures based on their academic nature and caseload. Geographically, the more JASTRO-certified physicians there were in a given area, the more radiation therapy tended to be used for cancer patients. In conclusion, the Japanese structure has clearly improved during the past 19 years in terms of equipment and its use, although a shortage of manpower and variations in maturity disclosed by PCS stratification remained problematic in 2009.

Keywords: Structure survey; radiotherapy facility; radiotherapy personnel; radiotherapy equipment; caseload

INTRODUCTION

The medical care systems of the USA and Japan have very different backgrounds. In 1990, the Patterns of Care Study (PCS) conducted a survey of the structure of radiation oncology facilities in 1989 for the entire census of facilities in the USA [1]. In 1991, the Japanese Society for Therapeutic Radiation Oncology (JASTRO) conducted the first national survey of the structure of radiation therapy facilities in Japan based on their status in 1990, and the results were reported by Tsunemoto *et al.* [2]. The first comparison of these two national structure surveys to illustrate and identify similarities and differences in 1989–90 was conducted by the author and reported in 1996 [3]. The resultant international exchange of information proved especially valuable for Japan, where the structure of radiation oncology could be improved on the basis of those data.

The Japanese structure has gradually changed since a greater number of cancer patients are treated with radiation and public awareness of the importance of radiotherapy (RT) has grown. JASTRO has conducted national structure surveys every two years since 1990 [2] and every year since 2011. Furthermore, in 2006 the Cancer Control Act was approved in Japan, which strongly advocates the promotion of RT and an increase in the number of radiation oncologists (ROs) and medical physicists. The Japanese Ministry of Education, Sciences and Sports is supporting the education of these specialists at university medical hospitals. The findings of international comparisons and the consecutive structural data gathered and published by JASTRO have been useful for an understanding of our current position and future direction [4–7]. In this report, the recent structure of radiation oncology in Japan is analyzed and compared with the data of 2007 [6].

MATERIALS AND METHODS

From March 2010 to January 2011, JASTRO conducted a questionnaire based on the national structure survey of radiation oncology in 2009. The questionnaire dealt with the number of treatment systems by type, number of personnel by category and number of patients by type, site and treatment modality. To measure variables over a longer period of time, data for the calendar year 2009 were also requested. The response rate was 700 out of 770 (90.6%) of active facilities. The data from 241 institutions (31.3%) were also registered in the International Directory of Radiotherapy Centres (DIRAC) in Vienna, Austria in 2011.

The PCS was introduced in Japan in 1996 [8–17]. The Japanese PCS employed methods similar to those of the American version, which used structural stratification to analyze national averages for the data for each survey item by means of two-stage cluster sampling. For the regular structure survey, RT facilities throughout the country were stratified into four categories. This stratification was based on academic conditions and the annual number of patients treated with radiation at each institution, because academic institutions require and have access to more resources for education and training, while the annual caseload also constitutes essential information related to structure. For the study reported here, the following institutional stratification was used. A1: university hospitals/cancer centers treating 462 patients or more per year; A2: the same type of institutions treating 461 patients or fewer per year; B1: other national/public hospitals treating 158 patients or more per year; and B2: other national hospital/public hospitals treating 157 patients or fewer per year.

SAS 8.02 (SAS Institute Inc., Cary, NC, USA) [18] was used for statistical analyses and statistical significance was tested by means of the chi-squared test, Student's *t*-test or analysis of variance (ANOVA).

RESULTS

Current situation of radiation oncology in Japan

Table 1 shows that the numbers of new patients and total patients (new plus repeat) undergoing radiation in 2009 were estimated at 201 000 and 240 000, respectively, showing a 11.0% increase over 2007 [6], with 40% of the patients being treated at academic institutions (categories A1 and A2), even though these academic institutions constituted only 20% of the 700 radiotherapy facilities nationwide.

Cancer incidence in Japan in 2009 was estimated at 724 426 cases [19] with approximately 27.6% of all newly diagnosed patients treated with radiation. This number and corresponding rate have increased steadily over the last 19 years and is expected to increase further [14]. In 1990, the rate was estimated to be approximately 15% [3], and it was 16% in 1995, 17% in 1997, 20% in 1999, 22% in 2001, 23.3% in 2003 [4], 24.5% in 2005 [5], 26.1% in 2007 [6] and 27.6% in 2009.

Facility and equipment distribution patterns

Table 2 shows an overview of RT equipment and related functions. There were 816 Linac, 46 Gamma Knife, 29 ^{60}Co remote afterloading system (RALS), 130 ^{192}Ir and 1 ^{137}Cs RALS systems in actual use, as well as 9 of the 15 telecobalt systems installed. The Linac systems used dual energy function for 586 (71.8%), 3D conformal radiation therapy (3DCRT) for 663 (81.3%) and intensity-modulated radiation therapy (IMRT) for 337 units (41.3%). The IMRT function was employed more frequently for the equipment of academic institutions (A1: 73.4% and A2: 49.5%) than that of non-academic institutions (B1: 42.3% and B2: 18.1%). However, 3DCRT functions were disseminated widely in both academic and non-academic institutions, with 69% even in B2 institutions. The use of image-guided radiation

Table 1. PCS stratification of radiotherapy facilities in Japan

Institution category	Description	Facilities (*n*)	New patients (*n*)	Average new patients/facility[a] (*n*)	Total patients (new + repeat) (*n*)	Comparison with data of 2007[b] (%)	Average total patients/facility[a] (*n*)	Comparison with data of 2007[b] (%)
A1	UH and CC (≥462 patients/y)	70	52 078	744.0	62 124	2.9	887.5	4.3
A2	UH and CC (<462 patients/y)	70	18 842	269.2	22 717	3.9	324.5	5.4
B1	Other (≥158 patients/y)	280	84 938	303.4	101 730	8.0	363.3	11.1
B2	Other (<158 patients/y)	280	26,532	94.8	31 258	9.2	111.6	13.5
Total		700	182 390[c]	260.6	217 829[c]	6.2	311.2	9.4
						7.3		5.9

PCS = Patterns of Care Study; UH = university hospital; CC = cancer center hospital; Other = other national, city, or public hospital.

[a] $P < 0.0001$.

[b] Rate of increase compared with the data of 2007. Calculating formula: $\frac{data\ of\ 2009\ (n) - data\ of\ 2007(n)}{data\ of\ 2007(n)} \times 100\ (\%)$

[c] Number of radiotherapy institutions was 770 in 2009, and the number of new patients was estimated at approximately 201 000; the corresponding number of total patients (new plus repeat) was 240 000.

therapy (IGRT) has been steadily expanding from A1 institutions (30.4% to 33.5%) to the other types of institutions (14.0% to 35.5%). The annual numbers of patients/Linac were 393.2 for A1, 244.3 for A2, 339.1 for B1 and 118 for B2 institutions and showed a 9.8 % increase compared with the data from 2007. The number of institutions with teleco-balt in actual use showed a major decrease to 9 and became stable compared with 2007. Gamma Knife was installed more frequently in B1 and B2 institutions. A significant replacement of ^{60}Co RALS with ^{192}Ir RALS was observed especially in academic institutions, while the number of new ^{60}Co RALS-type systems in use did not increase. Six particle machines were registered in this survey, two with carbon-beam and five with proton-beam irradiation. One machine in Hyogo Prefecture can deliver either carbon or proton beams. Although the HIMAC in Chiba Prefecture has two synchrotrons, it was registered as one machine in the 2009 survey. The total number of new cancer patients treated at these six institutions was estimated at 2038 (1.19% of all new patients in Japan). Twenty-seven advanced institutions were included in the A1 category and treated more than 800 patients per year. They were equipped with Linacs with dual energy (75.3% of the institutions), 3DCRT (97.2%) and IMRT function (82.2%), as well as with ^{192}Ir RALS (92.6%) and a computed tomography (CT) simulator (96.3%).

Table 3 shows an overview of RT planning and other equipment. X-ray simulators were installed in 51.6% of all institutions, and CT simulators in 82.1%, with the latter exceeding the former for the first time in 2007. There was a significant difference in the rate of CT simulators installed by institutional stratification, from 95.7% in A1 to 69.3% in B2 institutions. Very few institutions (16 institutions) used magnetic resonance imaging (MRI) for RT only, while computers were widely used for RT recording.

Staffing patterns and patient loads

Table 4 shows the staffing patterns and patient loads by institutional stratification. 'Full-time or part-time' refers to the style of employment. Since even full-time ROs must share the diagnosis in a week at smaller institutions such as found in the B2 category, we felt that these numbers were not adequate for an accurate evaluation of man power. Therefore, data for full-time equivalent (FTE: 40 h/week for radiation oncology service only) were assessed in terms of the clinical working hours in RT of each individual. This is thus a method to determine actual man power at each institution. The total number of FTE ROs in Japan stood at 939.4, while the average numbers were 4.6 for A1, 1.6 for A2, 1.3 for B1 and 0.6 for B2 institutions. The number in B1 improved by 30% compared with 2007 [6]. The overall patient load per FTE RO in Japan was 231.9, and for A1, A2, B1 and B2 institutions the loads were 193.5, 205.2, 290.6 and 198.4, respectively, with the patient load for B1 institutions being by far the highest. The increase in the overall patient load per

Table 2. Equipment, its function and patient load per equipment by PCS institutional stratification

Radiotherapy equipment and its function	A1 ($n=70$)		A2 ($n=70$)		B1 ($n=280$)		B2 ($n=280$)		Total ($n=700$)		Comparison with data of 2007 (%)
	n	%	*n*	%	*n*	%	*n*	%	*n*	%	
Linear accelerator	158		93		300		265		816		1.1[a]
with dual energy function	122	*77.2*[b]	70	*75.3*[b]	235	*78.3*[b]	159	*60.0*[b]	586	*71.8*[b]	5.0[c]
with 3DCRT function (MLC width ≥1.0 cm)	150	*94.9*[b]	81	*87.1*[b]	247	*82.3*[b]	185	*69.8*[b]	663	*81.3*[b]	12.5[c]
with IMRT function	116	*73.4*[b]	46	*49.5*[b]	127	*42.3*[b]	48	*18.1*[b]	337	*41.3*[b]	12.2[c]
with cone beam CT or CT on rail	48	*30.4*[b]	33	*35.5*[b]	73	*24.3*[b]	41	*15.5*[b]	195	*23.9*[b]	
with treatment position verification system (X-ray perspective image)	51	*32.3*[b]	31	*33.3*[b]	85	*28.3*[b]	37	*14.0*[b]	204	*25.0*[b]	
with treatment position verification system (other than those above)	53	*33.5*[b]	18	*19.4*[b]	77	*25.7*[b]	55	*20.8*[b]	203	*24.9*[b]	
Annual no. patients/Linac	393.2[d]		244.3[d]		339.1[a]		118.0[d]		266.9[d]		9.8[a]
Particle	3		0		3		0		6		
Microtoron	6		2		3		4		15		
Telecobalt (actual use)	2 (0)		2 (0)		3 (1)		8 (7)		15 (9)		
Gamma knife	3		2		32		9		46		
Other accelerator	2		1		1		1		5		
Other external irradiation device	4		2		1		0		6		
New type ^{60}Co RALS (actual use)	4 (4)	5.7[e] (5.7)	1 (1)	1.4[e] (1.4)	9 (9)	3.2[e] (3.2)	2 (1)	0.7[e] (0.4)	16 (15)	2.3[e] (2.1)	
Old type ^{60}Co RALS (actual use)	2 (2)	2.9[e] (2.9)	2 (1)	2.9[e] (1.4)	14 (11)	5.0[e] (3.9)	4 (0)	1.4[e] (0.0)	22 (14)	3.1[e] (2.0)	
^{192}Ir RALS (actual use)	60 (60)	85.7[e] (85.7)	32 (31)	45.7[e] (44.3)	37 (37)	13.2[e] (13.2)	4 (2)	1.4[e] (0.7)	133 (130)	19.0[e] (18.6)	
^{137}Cs RALS (actual use)	1 (0)		0 (0)		1 (1)		0 (0)		2 (2)		

PCS = Patterns of Care Study; RT = radiotherapy; 3D-CRT = three-dimensional conformal radiotherapy; MLC = multileaf collimator; IMRT = intensity-modulated radiotherapy; RALS = remote-controlled after-loading system.

[a]Rate of increase compared with the data of 2007. Calculating formula: $\frac{data\ of\ 2009\ (n) - data\ of\ 2007\ (n)}{data\ of\ 2007\ (n)} \times 100\ (\%)$

[b]Percentage calculated from the number of systems using this function and the total number of linear accelerator systems.

[c]Comparison with the data of 2007. Calculating formula: *data of* 2009 (%) − *data of* 2007 (%)

[d]The number of patients over the number of linear accelerators; institutions without linear accelerators excluded from calculation.

[e]Rate of institutions that have this equipment (≥2 pieces of equipment per institution).

Table 3. Radiotherapy planning and other equipments by PCS institutional stratification

RT planning and other equipment	A1 ($n=70$)		A2 ($n=70$)		B1 ($n=280$)		B2 ($n=280$)		Total ($n=700$)		Comparison with data of 2007[b] (%)
	n	%[a]	*n*	%[a]	*n*	%[a]	*n*	%[a]	*n*	%[a]	
X-ray simulator	55	74.3	41	55.7	130	46.1	135	48.2	361	50.7	−10.2
CT simulator	74	95.7	61	84.3	235	78.6	205	69.3	575	77.1	11.5
RTP computer (two or more)	340 (63)	100 (90.0)	167 (35)	100 (50.0)	461 (99)	97.5 (35.4)	303 (37)	92.5 (13.2)	1271 (234)	96.0 (33.4)	0.7 (10.1)
MRI (two or more)	201 (60)	95.7 (85.7)	151 (56)	98.6 (80.0)	504 (184)	97.5 (65.7)	364 (86)	97.9 (30.7)	1220 (386)	97.6 (55.1)	1.8 (3.8)
for RT only	2	2.9	2	2.9	9	2.9	3	1.1	16	2.1	0.6
Computer use for RT recording	64	91.4	65	92.9	264	94.3	238	85.0	631	90.1	1.3

CT = computed tomography; RTP = radiotherapy planning; MRI = magnetic resonance imaging; other abbreviations as in Table 2.
[a]Ratio of institutions that have equipment (≥2 pieces of equipment per institution).
[b]Comparison with the data of 2007. Calculating formula: *data of* 2009 (%) − *data of* 2007 (%).

FTE RO was 13.7% compared with 2007 (6). In Japan, 42.6 % of the institutions providing RT have their own designated beds, where ROs must also take care of their in-patients. The percentage distribution of institutions by patient load per FTE RO shown in Fig. 1a indicates that the largest number of facilities featured a patient/FTE staff level in the 101–150 range, and in the 151–200 range for the second largest number. The blue areas of the bars show that 47.7% of the institutions (334/700) had less than one FTE RO. Compared with 2007 [6], the patient load has increased even more.

A similar trend was observed for RT technologists and their patient load by institutional stratification with the percentage distribution of institutions by patient load per radiation technologist displayed in Fig. 1b. The largest number of facilities had a patient-per-radiotherapy technologist level in the 101–120 range, with the second largest number showing a range of 81–100 and the third largest a range of 121–140. There were 113.1 FTE medical physicists, 113.1FTE radiotherapy quality assurance (QA) staff and 1836FTE radiotherapists. For this survey, personnel numbers were checked for duplicate reporting by identification of individuals on staffing data and these data were analyzed in detail in another report [7]. Finally, there were 621.2 FTE nurses.

Distribution of primary sites, specific treatment and palliative treatment

Table 5 shows the distribution of primary sites by institutional stratification. The most common disease site was the breast, followed by the lung/bronchus/mediastinum and genito-urinary region. In Japan, the number of patients with prostate cancer undergoing RT was 17 919 in 2009, showing an increase of 10.4% over 2007 [6]. By disease site, the rate of increase compared with 2007 was the highest for prostate cancer at 10.4%, the second highest for breast cancer at 9.6% and the third highest for head and neck cancer at 9.3%. The stratification of institutions indicates that the rate of increase for lung cancer was notable for A1 institutions and the rates for prostate cancer were high for all categories, ranging from 8.0–20.3%. On the other hand, the rate for breast cancer was the lowest (–0.7%) for A2, while those for B1 and B2 ranged from 11.8–18.8%, and the rates for head and neck cancer were high for A2 (17.7%) and B1 (21.4%).

Table 6 shows the distribution of use of specific treatments and the number of patients treated with these modalities by PCS stratification of institutions. Use of interstitial irradiation, radioactive iodine therapy for prostate cancer, stereotactic body RT, IMRT and hyperthermia increased by 23.3%, 14.5%, 4.9%, 34.8% and 15%, respectively, compared with 2007 [6]. On the other hand, the use of intraoperative RT decreased significantly by –31.1%. Institutional stratification shows that there was a dramatic increase of 454.1% in the use of IMRT in B2 [5]. In 2009,

Table 4: Structure and personnel by PCS institutional stratification

	Structure and personnel					
	A1 (*n* = 70)	**A2** (*n* = 70)	**B1** (*n* = 280)	**B2** (*n* = 280)	**Total** (*n* = 700)	**Comparison with data of 2007 [a] (%)**
Institutions/total institutions (%)	10.0	10.0	40.0	40.0	100	-
Institutions with RT bed (*n*)	59 (84.3)	37 (52.9)	124 (44.3)	78 (27.9)	298 (42.6)	6.0 (3.6 [b])
Average RT beds/institution (*n*)	11.2	3.3	3.1	1.5	3.3	6.5
Number of ROs (full time + part time)	369 + 64	151 + 35	372 + 216	193 + 245	1085 + 560	6.7
JASTRO-certified RO (full time)	214	73	192	52	531	11.3
Average JASTRO-certified RO/institution (*n*)	3.1	1.0	0.7	0.2	0.8	14.2
Total (full-time and part-time) RO FTE*	321.1	110.7	350.1	157.5	939.4	13.7
Average FTE ROs/institution	4.6	1.6	1.3	0.6	1.3	18.2
Patient load/FTE RO	193.5	205.2	290.6	198.4	231.9	-6.7
Number of RT technologists (full time + part time)	492 + 22	280 + 13	1133 + 33	825 + 2	2730 + 70	4.4
Total (full-time and part-time) RT technologist FTE	434.3	206.8	758.6	436.2	1836.0	12.4
Average FTE RT technologists/institution	6.2	3.0	2.7	1.6	2.6	13.0
Patient load/FTE RT technologist	143.0	109.9	134.1	71.7	118.6	-5.5
Number of full-time nurse (full time + part time)	114 + 26	74 + 13	270 + 82	125 + 50	583 + 171	-37.1
Total (full-time and part-time) nurse FTE	135.4	68.7	290.4	126.8	621.2	25.6
Number of medical physicists (full time + part time)	70 + 5	27 + 2	125 + 10	65 + 5	287 + 22	10.8
Total (full-time and part-time) medical physicist FTE	32.3	8.7	54.4	22.0	117.6	71.9
Number of RT QA staffs (full time + part time)	79 + 0	52 + 0	174 + 3	85 + 3	390 + 6	-26.1
Total (full-time and part-time) RT QA staff FTE	25.8	15.2	50.3	25.0	116.3	9.1

JASTRO = Japanese Society of Therapeutic Radiation Oncology; RO = radiation oncologist; FTE = full-time equivalent (40 h/wk only for RT practice); QA = quality assurance; other abbreviations as in Table 2. RT QA staff: Japanese Organization of RT Quality Management has certified RT quality managers from RT technologist since 2005 mainly by educational session.Data in parentheses are percentages.

[a]Rate of increase compared with the data of 2007. Calculating formula: $\frac{data\ of\ 2009\ (n) - data\ of\ 2007\ (n)}{data\ of\ 2007\ (n)} \times 100\ (\%)$

[b]Comparison with the data of 2007. Calculating formula: *data of* 2009 (%) − *data of* 2007 (%)

101 institutions (14.4%) actually utilized IMRT, which was significantly lower than the 337 Linacs with IMRT function (41.3%) as shown in Table 2. Figure 2 lists the numbers of patients treated with SRT and IMRT for each survey year. Approximately 12 000 patients were treated with SRT for the brain in each survey year and this number has remained stable. On the other hand, the number treated with SRT for the rest of the body has been increasing gradually and exceeded 2000 in 2009. The corresponding number of patients for IMRT has been increasing more rapidly and exceeds 4000, or about 2% of all RT-treated patients in 2009.

Table 7 shows the number of patients with brain or bone metastasis treated with radiation according to the same institutional stratification. More patients with brain metastasis (12.2% of all patients) were treated at B1 than at the other types of institutions, while use of radiation for bone